APPLIED AND ENVIRONMENTAL MICROBIOLOGY, Feb. 1992, p. 600–606
0099-2240/92/020600-07$02.00/0

Vol. 58, No. 2

Bacterial Oxidation of Sulfide Minerals in Column Leaching Experiments at Suboptimal Temperatures

LASSE AHONEN[1]† AND OLLI H. TUOVINEN[2]*

Department of Microbiology, University of Helsinki, SF-00710 Helsinki, Finland,[1] and Department of Microbiology, The Ohio State University, 484 West 12th Avenue, Columbus, Ohio 43210-1292[2]

Received 10 August 1991/Accepted 26 November 1991

The purpose of the work was to quantitatively characterize temperature effects on the bacterial leaching of sulfide ore material containing several sulfide minerals. The leaching was tested at eight different temperatures in the range of 4 to 37°C. The experimental technique was based on column leaching of a coarsely ground (particle diameter, 0.59 to 5 mm) ore sample. The experimental data were used for kinetic analysis of chalcopyrite, sphalerite, and pyrrhotite oxidation. Chalcopyrite yielded the highest (73 kJ/mol) and pyrrhotite yielded the lowest (25 kJ/mol) activation energies. Especially with pyrrhotite, diffusion contributed to rate limitation. Arrhenius plots were also linear for the reciprocals of lag periods and for increases of redox potentials (dmV/dt). Mass balance analysis based on total S in leach residue was in agreement with the highest rate of leaching at 37 and 28°C. The presence of elemental S in leach residues was attributed to pyrrhotite oxidation.

Biological leaching processes for metal recovery are based on the bacterial oxidation of sulfide minerals, basically involving ferrous iron and various inorganic sulfur compounds as the electron donors (9, 14). These processes are used on a commercial scale in dump leaching operations for Cu recovery (12) and in tank leaching for the pretreatment of refractory, pyrite- and arsenopyrite-containing gold ores (10). Although biological leaching rates are greatly influenced by the prevailing temperatures, relatively little is known about the temperature limitation on the bacterial oxidation of the various sulfide minerals in leaching operations. Temperatures of open mine waters and leach solutions display seasonal changes in surface heaps, whereas underground leach circuits are characterized by relatively constant temperatures. Sulfide ores are potential heat sources, but little is known about temperature distribution in existing heap leaching systems. Elevated temperature zones within ore piles have been reported. In general, however, temperature distribution is highly variable in leach mines. Mesophilic bacteria active in leach mines, namely, *Thiobacillus ferrooxidans* and *Leptospirillum ferrooxidans*, can function at temperatures up to about 40°C, above which they show thermal responses such as rapid expression of heat shock proteins and loss of normal cellular activities, including carbon dioxide fixation (6, 8). Moderately thermophilic acidophiles are active in the temperature range between 40 and 60°C, and thermophilic bacteria (e.g., *Sulfobacillus*, *Acidianus*, and *Sulfolobus* spp.) can thrive at temperatures up to 80°C (11). In the lower-temperature range, iron-oxidizing thiobacilli continue to be metabolically active at 2 to 4°C, but they display temperature optima in the mesophilic range of around 30 ± 3°C (1, 3, 7). Biological oxidation of sulfur displays a similar temperature response (4). Truly psychrophilic bacteria have not been characterized from biological leaching operations.

In the present work, the biological leaching characteristics of a high-grade sulfide ore material were evaluated over a temperature range of 4 to 37°C. The experimental technique was based on column leaching, involving coarsely ground materials and time courses lasting more than 1 year. Finely ground ore material from the same source was previously evaluated in short-term experiments with a shake flask technique (5). For this report, the temperature relationships were quantitated for the bacterial oxidation of the sulfide minerals occurring in the sample. Mass balances for sulfur and metals were also determined at the termination of the leaching tests.

MATERIALS AND METHODS

The ore material was the same as in the previously reported shake flask experiments (5). The sample was ground and sieved to a particle size of 0.59 to 5 mm, and it had the following average chemical composition on the basis of four replicate 400-g samples (percentages are wt/wt): Cu, 6.0%; Zn, 0.4%; Ni, 0.078%; Co, 0.62%; Fe, 37.8%; total S, 35.7%. The sample contained approximately 40% pyrite, 20% pyrrhotite, 17% chalcopyrite, 0.4% Co,Ni-pentlandite (Co/Ni, ~1:1), and 0.7% sphalerite. Pyrite contained 0.6% Co and 0.02% Ni. Pyrrhotite contained 0.03% Co and 0.3% Ni.

Each air lift column was charged with 400 g of ore sample and 800 ml of mineral salts solution [0.4 g each of $(NH_4)_2SO_4$, K_2HPO_4, and $MgSO_4 \cdot 7H_2O$ per liter]. The samples were initially preleached with frequent pH adjustment for 2 days without bacteria to neutralize alkaline materials before the leaching was started by addition of 50 ml of a composite mine water sample. This composite sample originated from a copper mine (3) and served as an inoculum for all columns. The leach solution was collected at the bottom of the column and was continuously recirculated by raising it to the top of the column with an air lift side arm. The columns were held at 4, 7, 10, 13, 16, 19, 28, 37, and 46°C. The column leaching experiment at 46°C was discontinued after several months because of the lack of bacterial activity.

The leaching was monitored by measurement of pH, redox

* Corresponding author.
† Present address: The Geological Survey of Finland, SF-02150 Espoo, Finland.

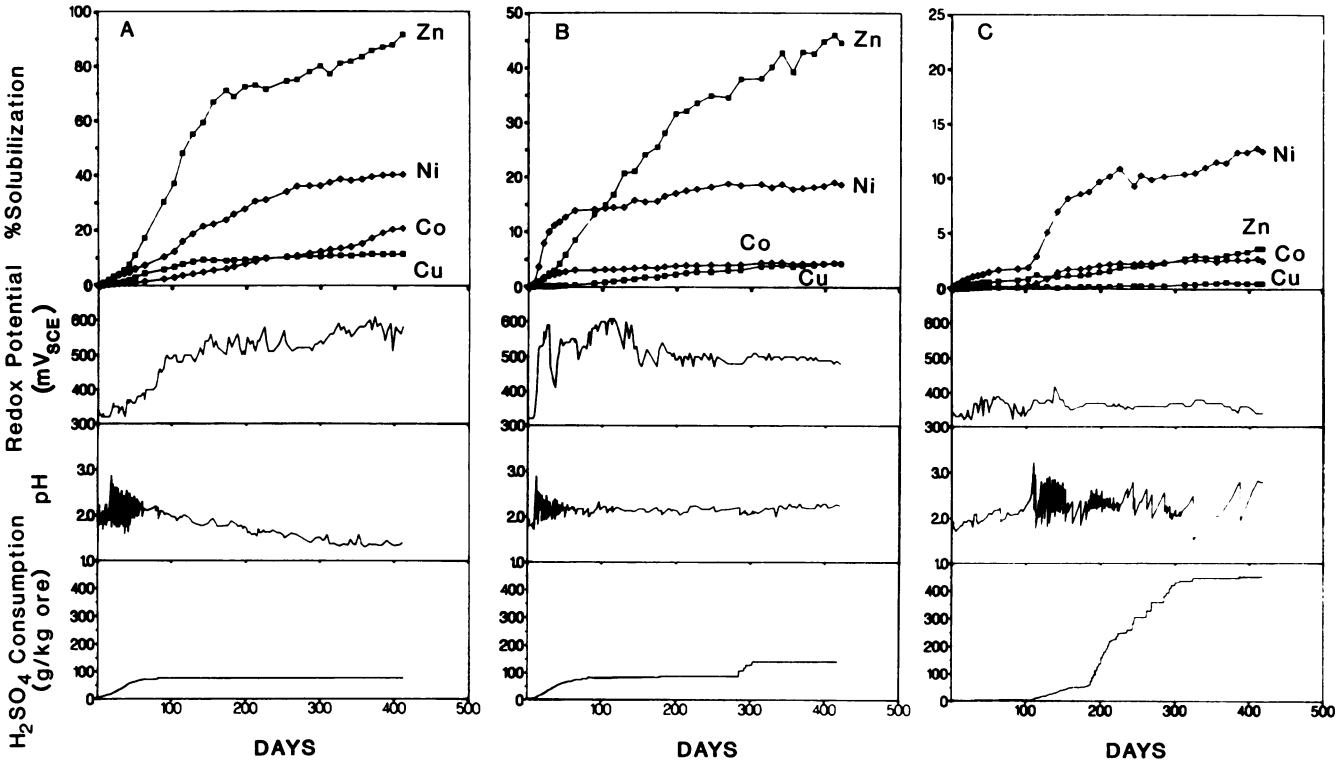

FIG. 1. Column leaching at (A) 37°C, (B) 19°C, and (C) 4°C. Solubilization of Cu, Co, Ni, and Zn from the ore, redox potential, pH, and acid consumption are given. SCE, standard calomel electrode. Note the difference in scale in the top panels in A, B, and C.

potential, and dissolved metals. Redox potential measurements (Pt electrode) were referenced against a standard calomel electrode. Samples of leach solutions were replaced with equal volumes of sterile mineral salts solution; the results have been corrected for this dilution effect. Cumulative acid consumption was calculated on the basis of the amount of sulfuric acid added for pH adjustment. Evaporation was estimated on a volumetric basis and compensated for by adding sterile, distilled water.

The concentrations of dissolved metals were measured with atomic absorption spectrometry. At the termination of the experiments, leaching residues were air dried and weighed. The elemental composition of solids was determined with both atomic absorption spectrometry and X-ray fluorescence spectrometry. Total sulfur was determined by X-ray fluorescence spectrometry or by conversion to SO_2 (induction furnace) followed by infrared detection. Elemental sulfur was determined by iodometric titration. Sulfate in leach solution was determined indirectly with excess $BaCl_2$ addition followed by atomic absorption spectrometry.

As in our previous report (5), kinetic evaluation was based on rate determinations, using a shrinking-particle model and a shrinking-core model. Fundamentals of these models have been discussed by Sohn and Wadsworth (13, 15). Both models were simplified to rate expressions that could be used to linearize the data for rate calculations.

In the simplified shrinking-particle model, the rate constant (k) is expressed as $k = \{\ln [W_0/(W_0 - y)]\}/t$, where W_0 is the initial metal content in the ore sample, y is the amount of metal in solution, and t is time. This model predicts that the leaching rate is proportional to the residual mass of the mineral. The respective half-lives were calculated from the rate constants as $\ln 2/k$.

In the shrinking-core model, the rate constant is expressed as $k = y/\sqrt{t}$, which indicates a parabolic relation between the amount of metal in solution and the time. The leaching rate is inversely proportional to the concentration of the dissolved metal. The times required for 25, 50, and 90% leaching were thus calculated from the respective rate constants as y^2/k^2.

RESULTS AND DISCUSSION

Acid consumption. Time courses of leaching experiments at three different temperatures are presented in Fig. 1. The acid demand was not satisfied during the preleaching period and necessitated periodic pH adjustments of the leach solutions to maintain the pH below 2.2. Also, acid consumption was associated with the beginning of active leaching (Fig. 1A to C). As the leaching progressed, the acid demand decreased. Acid production due to the bacterial leaching became gradually sufficient only at 37°C and decreased the pH to 1.5 (Fig. 1A). At lower temperatures, acid consumption continued to exceed acid production. Acid demand ranged between 90 and 450 g of sulfuric acid per kg of ore material, with columns held at the highest (37°C) and lowest (4°C) temperatures displaying the lowest and highest acid consumption, respectively.

Initially, the redox potentials were around 350 mV and increased to the 500- to 600-mV range during active leaching. At 4°C, the redox potential did not increase, suggesting that iron in solution was predominantly in the ferrous form (Fig. 1C).

Leaching of chalcopyrite. Chalcopyrite was virtually the exclusive copper mineral in this ore material, and secondary copper minerals were present in negligible amounts. The

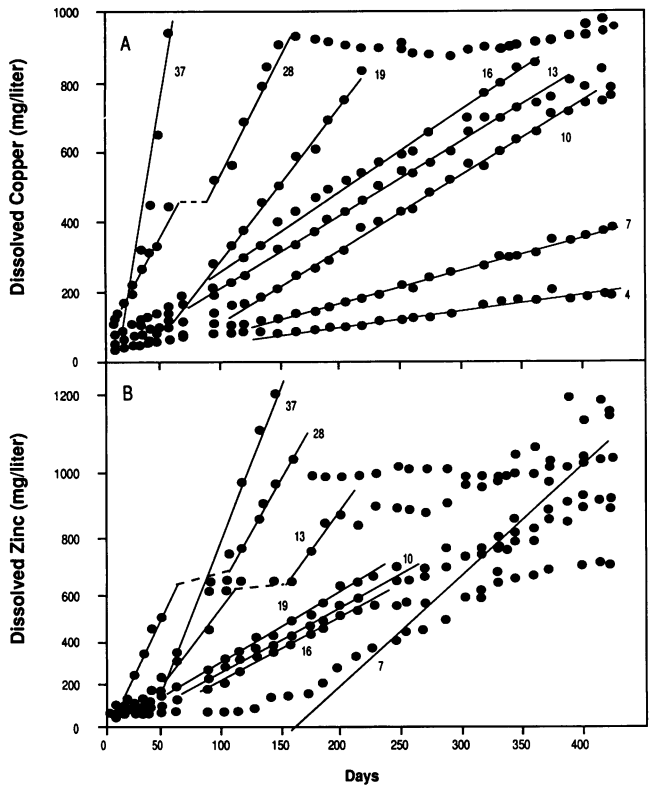

FIG. 2. Leaching (A) copper and (B) zinc at the test temperatures as a function of time on the basis of linearized plots [ln $W_0/(W_0 - y)$]. Two columns experienced interruptions, and the respective linear portions of the leach curves are connected with a broken line.

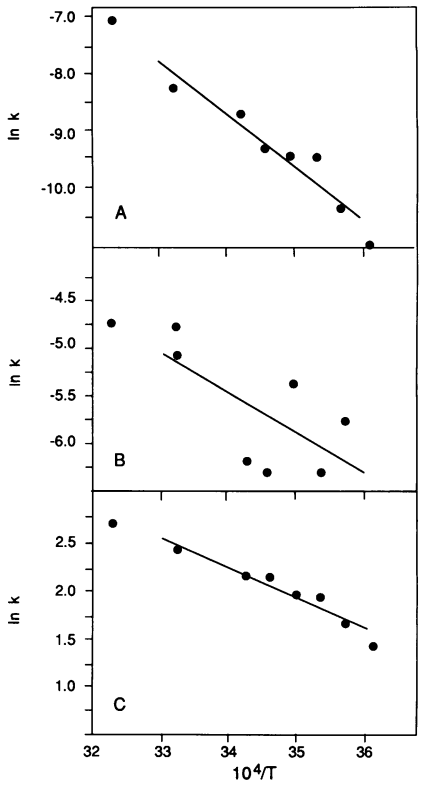

FIG. 3. Arrhenius plot of the bacterial leaching of (A) copper, (B) zinc, and (C) nickel.

increase in the concentration of copper displayed linearity during the leaching (Fig. 2A). At 28°C the leaching levelled off after 150 days, and subsequent concentrations slightly declined, suggesting copper precipitation. An Arrhenius plot yielded a linear relationship between the rate constants and test temperatures (Fig. 3A). The slope of the Arrhenius plot yielded an activation energy value of 73 kJ/mol for copper leaching. The kinetic parameters for the oxidation of the chalcopyrite are listed in Table 1.

Leaching of sphalerite. Sphalerite was the sole zinc mineral in this ore sample. The time courses of zinc solubilization at the test temperatures are shown in Fig. 2B. Rate data for leaching at 4°C could not be calculated because of the negligible leaching. The kinetic parameters of zinc solubilization are listed in Table 2. The Arrhenius plot of the rate constants (Fig. 3B) displayed more scatter than was found with chalcopyrite leaching. The plot yielded a tentative activation energy value of 35 kJ/mol.

Leaching of pyrrhotite, pentlandite, and pyrite. On the basis of the Ni content and the relative abundance of pyrrhotite and pentlandite, it was estimated that approximately 50% of the total nickel was associated with pyrrhotite. Mineralogical examinations of leach residues have revealed a preferential solubilization of pyrrhotite in relation to pentlandite. The initial solubilization of Ni was thus taken to represent the leaching of pyrrhotite.

After lag periods, nickel solubilization displayed a fast phase followed by a gradual decline as a function of time (Fig. 4A). These leach curves displayed linearity on parabolic plots (Fig. 4B). The kinetic parameters are listed in Table 3. An activation energy value of 25 kJ/mol was calculated from the respective Arrhenius plot (Fig. 3C).

Pentlandite (ca. 0.4% in the sample) was associated with pyrrhotite, and it was coleached during pyrrhotite oxidation. The molar proportion of cobalt and nickel [Co/(Co + Ni)]

TABLE 1. Kinetic parameters of copper leaching

Temp (°C)	Rate constant (1/day)	Correlation coefficient	Rate (%/yr)	Half-life (yr)
37	0.000757	0.984	28	2.5
28	0.000232	0.985	8.5	8.2
19	0.000149	0.997	5.4	13
16	0.0000785	0.994	2.9	24
13	0.0000701	0.998	2.6	27
10	0.0000705	0.998	2.6	27
7	0.0000310	0.994	1.1	61
4	0.0000154	0.983	0.56	120

TABLE 2. Kinetic parameters of zinc leaching

Temp (°C)	Rate constant (1/day)	Correlation coefficient	Rate (%/mo)	Half-life (yr)
37	0.00905	0.988	27	0.21
28	0.00629	0.996	19	0.30
19	0.00206	0.997	6.2	0.92
16	0.00185	0.995	5.6	1.00
13	0.00472	0.971	14	0.40
10	0.00188	0.993	5.6	1.00
7	0.00314	0.970	9.4	0.60

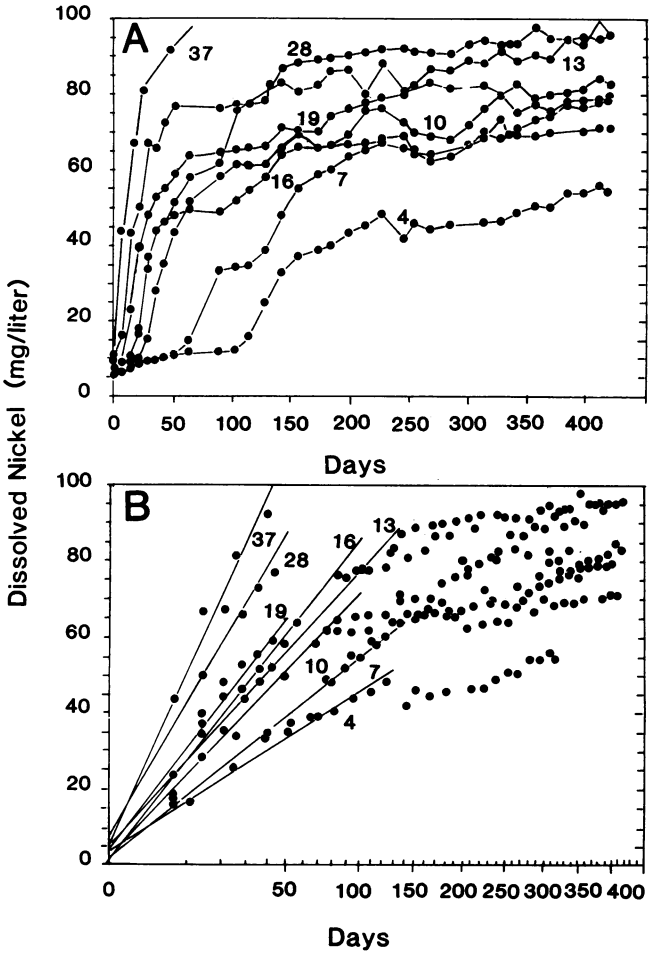

FIG. 4. Leaching of nickel at the test temperatures as a function of time on the basis of (A) concentration and (B) linearized (parabolic) plots.

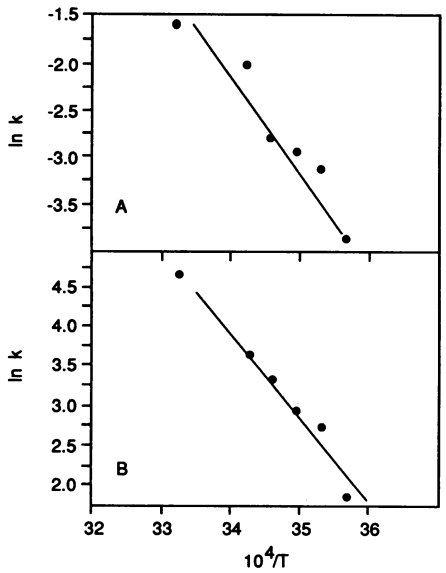

FIG. 5. Arrhenius plot based on (A) lag periods (1/day) preceding the active phase of bacterial leaching and (B) rate constants associated with increases in redox potentials.

was close to 0.67 and remained relatively constant during the leaching, except in the 37°C experiment in which cobalt was dissolved in increasing amounts relative to nickel. The relatively constant ratio of cobalt and nickel indicates a common source of the two metals, namely, Co,Ni-pentlandite. In addition, because acid production due to bacterial leaching was not apparent at temperatures other than 37°C, it was concluded that the main source of cobalt was the Co,Ni-pentlandite. The increasing concentration of Co at 37°C demonstrates the presence of an additional source of dissolved Co, namely, pyrite. Thus, except for the column at 37°C, relatively minor amounts of pyrite were dissolved in these experiments. The lack of significant pyrite oxidation was also supported by observations that acid consumption continued in all columns except at the highest test temperature, as shown in Fig. 1B and C for column leaching at 19 and 4°C.

TABLE 3. Kinetic parameters of nickel leaching

Temp (°C)	Rate constant (1/day)	Correlation coefficient	Calculated leaching time (yr)		
			$t_{25\%}$	$t_{50\%}$	$t_{90\%}$
37	0.0379	0.991	0.12	0.48	1.5
28	0.0290	0.979	0.20	0.81	2.6
19	0.0220	0.985	0.35	1.4	4.6
16	0.0216	0.980	0.37	1.5	4.8
13	0.0184	0.986	0.51	2.0	6.6
10	0.0178	0.987	0.54	2.2	7.0
7	0.0134	0.988	0.95	3.8	12
4	0.0107	0.990	1.5	6.0	19

Effect of temperature on bacterial activity. The progress of the bacterial leaching process was indicated by changes in pH and redox potential values (Fig. 1). At the beginning of the experiments, the pH remained constant until the acid consumption due to oxidation of monosulfides (mainly pyrrhotite) started. The concurrent oxidation of soluble ferrous iron was reflected in the increase of redox potential. A pronounced acidification of the solution due to the oxidation of pyrite was only observed at the highest temperature.

The lag periods were taken to parallel the phase of low redox potential. At the lower temperatures (7 and 4°C), the increase in redox potential was less pronounced than at higher temperatures. In this case, the lag periods were estimated to precede a rapid increase in acid consumption, coinciding with Ni and Zn leaching. Thus, iron remained mainly in the reduced form in the bacterial leaching at 4 and 7°C. At higher temperatures, acid consumption is more effectively neutralized by ferric iron hydrolysis and concurrent pyrite oxidation. At 37°C, the initial phase of increasing redox potential was prolonged, probably because of relatively fast reduction of ferric iron by sulfides.

Changes in the redox potential were also used to determine the length of the lag period at each test temperature. The lag periods were 5 days at 28°C, 7.5 days at 19°C, 16 days at 16°C, 19 days at 13°C, 23 days at 10°C, 53 days at 7°C, and 110 days at 4°C. Arrhenius plots of the inverse values of lag periods yielded a linear relationship (Fig. 5A) and an activation energy (E_a) value of 85.5 kJ/mol. The E_a thus derived is very similar to the value of 83 kJ/mol which was determined for ferrous sulfate oxidation with a sample

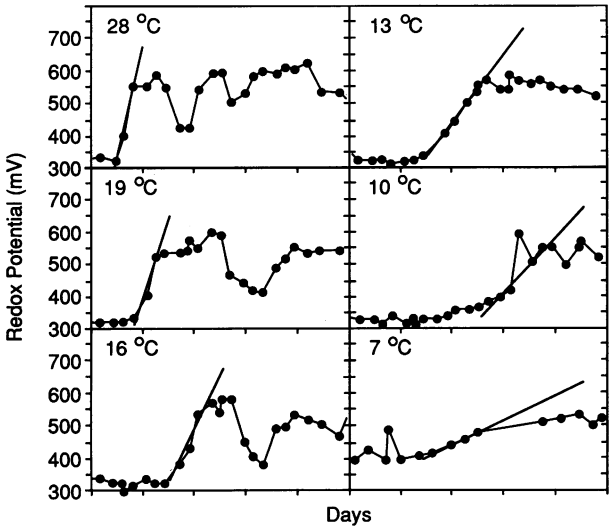

FIG. 6. Changes of redox potential values during incipient stages of bacterial leaching. For each test temperature, a 50-day period is shown in divisions of 10 days, displaying the first discernible increase in the millivolt scale. The time courses start from the beginning of each column leaching experiment (i.e., days 0 to 50), except the 7°C data, which are shown for days 43 to 93.

TABLE 5. Elemental distribution, expressed as percentage of the initial elemental content of the ore sample, in column leaching experiments

Element	Phase	% Distribution at given test temp							
		37°C	28°C	19°C	16°C	13°C	10°C	7°C	4°C
Cu	Solids	82	86	87	89	92	91	105	98
	Solution	11	3	4	3	3	2	1	1
	Sum	93	89	91	92	95	93	106	99
Zn	Solids	5	30	41	47	21	37	40	96
	Solution	92	52	45	36	58	46	56	4
	Sum	97	82	86	83	79	83	96	100
Ni	Solids	26	51	65	59	60	59	64	83
	Solution	40	21	19	16	23	19	18	13
	Sum	66	72	84	75	83	78	82	96
Co	Solids	63	88	93	90	93	95	96	100
	Solution	21	5	4	4	6	5	5	3
	Sum	84	93	97	94	99	100	101	103
Fe	Solids	59	66	71	78	66	75	69	77
	Solution	18	7	8	7	14	12	16	13
	Sum	77	73	79	85	80	87	85	90
S_{total}	Solids	76	82	92	93	80	93	92	94
$S_{sulfide}$	Solids	62	75	81	79	77	82	81	86

from the same source of mine water for initial enrichments (3).

Redox potentials sensitively reflected changes in the Fe^{3+}/Fe^{2+} ratios of dissolved iron in leach solution. The redox potential remained low at 4°C, but at all other test temperatures the redox potentials reached values of >500 mV. The increases in redox potential displayed linearity (Fig. 6), and the respective slopes were related to the temperature of incubation. Rate constants (dmV/dt) yielded a linear Arrhenius plot (Fig. 5B) and an activation energy value of 87 kJ/mol, which was comparable to the previous estimates based on either lag periods (85.5 kJ/mol) or direct measurements of bacterial iron oxidations (83 kJ/mol).

Leaching residues. The chemical composition of the solid residues and their respective weights are presented in Table 4. These data were further used for mass balance calculations, which are presented in Table 5. The yields of leaching estimated from the analyses of solid residues were generally in agreement with yields calculated from the concentrations of metals in solution.

The mass balances at the higher test temperatures displayed more deviation from the expected 100% compared with the data for the lower-temperature range. This may be partially attributed to the loss of metals caused by evaporation and splashing of the leach solution during recirculation, as evidenced by the formation of evaporative precipitates in the upper part of the column walls. Also, some loss of leach solution due to diffusion may have occurred around valves and fittings, which would have contributed to the elemental loss because of the long time course of >1 year.

The amount of sulfate added to the experimental columns in the form of sulfuric acid and mineral salts exceeded the amount of sulfate produced during the leaching. Therefore, a mass balance involving sulfate was not estimated. Total S in the solid residues was lowest in the 37°C sample, indicating the formation of soluble sulfate. A decreased residual sulfide content at 37 and 28°C was also apparent. Elemental S in the solid residues ranged between 10 and 18% of the total S, and this is largely attributed to pyrrhotite oxidation. Sulfur in the

TABLE 4. Partial analysis of leach residues

Test temp (°C)	Wt of solid residue (g)	% Composition by given method[a]										
		AAS						XRF				
		Cu	Zn	Ni	Co	Fe	S	Cu	Zn	Ni	Fe	S
37	326	5.74	0.024	0.030	0.480	26.8	34.5	6.32	0.024	0.019	27.9	31.8
28	337	6.12	0.144	0.052	0.644	31.2	36.9	6.18	0.145	0.042	27.6	33.0
19	383	5.60	0.170	0.064	0.604	30.5	37.0	5.30	0.172	0.042	25.7	31.4
16	393	5.52	0.190	0.050	0.570	30.1	35.1	5.30	0.193	0.043	29.9	32.3
13	369	6.00	0.088	0.054	0.626	28.4	37.4	6.01	0.095	0.048	25.7	33.2
10	388	5.92	0.154	0.054	0.610	31.6	36.5	5.29	0.148	0.041	26.9	31.9
7	369	6.90	0.170	0.062	0.642	29.4	38.1	6.76	0.180	0.046	26.8	33.4
4	369	6.44	0.414	0.084	0.670	32.7	38.5	6.29	0.419	0.056	30.2	34.1

[a] AAS, atomic absorption spectrometry; XRF, X-ray fluorescence spectrometry.

TABLE 6. Elemental composition of precipitate samples

Element	% Composition	
	Sample 1[a]	Sample 2[b]
Cu	1.32	4.22
Zn	0.19	0.30
Ni	0.038	0.062
Co	0.138	0.216
Fe	34.9	23.3
S_{total}	15.0	21.2
S^0	2.4	—[c]
S as sulfate	5.7	5.4
SiO_2	3.62	16.3
K_2O	0.64	1.97
P_2O_5	0.086	0.287
CaO	ND[d]	0.097
MgO	ND	3.8
C	0.44	3.8

[a] Composite sample from columns at 7 to 37°C.
[b] Sample from the column at 4°C.
[c] —, not analyzed.
[d] ND, not detected.

form of sulfate was present at 0.3 to 1.3% of the total S in the solid residues.

A small sample of residual precipitates was removed from each column for elemental analysis (Table 6). The samples were used as a composite except the sample from the 4°C column, which was analyzed separately (Table 6). The data indicated the presence of iron precipitates, which under these experimental conditions are primarily jarosites. Relative to their concentration in solution, the precipitates retained Cu more efficiently than Zn, Ni, or Co. Calcium sulfate was not a major product. The high C content in sample 2 is taken to represent carbonate fines.

Concluding remarks. The work presented herein should be construed as an empirical study of relative leaching rates of sulfide minerals in a mixed system. The results do not represent the E_a values of pure, single minerals because the interactions between various minerals cannot be ruled out. Although they cannot be discerned from the experimental results, it is possible that galvanic coupling effects caused by physical contact between different sulfide minerals were involved in influencing column leaching rates.

The activation energy values determined in this study, including results from our previous experiments, are summarized in Table 7. Activities related directly or indirectly to ferrous iron oxidation (i.e., Fe^{2+} oxidation, the resulting increase in redox potential, pyrite oxidation, and chalcopyrite oxidation) displayed comparable activation energy values, clearly in the range at which rate limitation is due to a chemical or biochemical reaction. Pyrrhotite oxidation displayed a considerably lower activation energy value, suggesting that rate control is primarily due to diffusion of reactants or products. Thus, an increase in the temperature would have a lesser effect on the rate of pyrrhotite leaching when contrasted with respective effects on pyrite or chalcopyrite leaching. However, the leaching rate of pyrrhotite is by far faster than that of pyrite or chalcopyrite. Pyrrhotite leaching creates a product zone, composed of a sulfur rim with a high content of elemental sulfur (2). A similar sulfur-containing layer is presumed to form on the chalcopyrite surface, especially during the ferric-iron-dependent leaching. This was not apparent in the present work since the data yielded a good linear fit with the modified shrinking-particle model. Overall, the chalcopyrite leaching rate was low, and it is possible that the oxidation of the other sulfide minerals masked kinetic effects caused by the formation of secondary layers.

TABLE 7. Activation energy values based on the present work and previously published data (3–5)

Reaction	E_a (kJ/mol)	
	Shake flask bioleaching expt	Column bioleaching expt
Fe^{2+} oxidation	83	—[a]
Sulfur oxidation	63	—
Pyrite oxidation	64	—
Chalcopyrite oxidation	77	73
Sphalerite oxidation	45	35
Pyrrhotite oxidation	40	25
1/lag period	—	86
Redox potential	—	87

[a] —, not determined.

ACKNOWLEDGMENTS

We thank P. Hietanen for technical assistance.

The work was partially funded by the Ministry of Trade and Industry (Finland), Outokumpu Research Ltd., and the Nordisk Industrifond.

REFERENCES

1. **Ahonen, L., P. Hietanen, and O. H. Tuovinen.** 1990. Temperature relationships of iron-oxidizing bacteria, p. 21–28. *In* G. I. Karavaiko, G. Rossi, and Z. A. Avakyan (ed.), International seminar on dump and underground bacterial leaching of metals from ores. Centre for International Projects, USSR Commission for UNEP, Moscow.
2. **Ahonen, L., P. Hiltunen, and O. H. Tuovinen.** 1986. The role of pyrrhotite and pyrite in the bacterial leaching of chalcopyrite ores, p. 13–22. *In* R. W. Lawrence, R. M. R. Branion, and H. G. Ebner (ed.), Fundamental and applied biohydrometallurgy. Elsevier Science Publishers, Amsterdam.
3. **Ahonen, L., and O. H. Tuovinen.** 1989. Microbiological oxidation of ferrous iron at low temperatures. Appl. Environ. Microbiol. **55**:312–316.
4. **Ahonen, L., and O. H. Tuovinen.** 1990. Kinetics of sulfur oxidation at suboptimal temperatures. Appl. Environ. Microbiol. **56**:560–562.
5. **Ahonen, L., and O. H. Tuovinen.** 1991. Temperature effects on bacterial leaching of sulfide minerals in shake flask experiments. Appl. Environ. Microbiol. **57**:138–145.
6. **Alvarez, S., and C. A. Jerez.** 1990. Molecular aspects of the stress response in *Thiobacillus ferrooxidans* and other biomining microorganisms, p. 439–449. *In* J. Salley, R. G. L. McCready, and P. L. Wichlacz (ed.), Biohydrometallurgy. Canada Centre for Mineral and Energy Technology, Ottawa, Ontario.
7. **Ferroni, G. D., L. G. Leduc, and M. Todd.** 1986. Isolation and temperature characterization of psychrotrophic strains of *Thiobacillus ferrooxidans* from the environment of a uranium mine. J. Gen. Appl. Microbiol. **32**:169–175.
8. **Jerez, C. A.** 1988. The heat shock response in meso- and thermoacidophilic chemolithotrophic bacteria. FEMS Microbiol. Lett. **56**:289–294.
9. **Kelley, B. C., and O. H. Tuovinen.** 1988. Microbiological oxidations of minerals in mine tailings, p. 33–53. *In* W. Salomons and U. Förstner (ed.), Chemistry and biology of solid waste: dredged material and mine tailings. Springer-Verlag KG, Berlin.
10. **Lindström, E. B., E. Gunneriusson, and O. H. Tuovinen.** 1992. Bacterial oxidation of refractory sulfide ores for gold recovery. Crit. Rev. Biotechnol. **12**:133–155.
11. **Norris, P. R.** 1990. Acidophilic bacteria and their activity in

mineral sulfide oxidation, p. 3–27. *In* H. L. Ehrlich and C. L. Brierley (ed.), Microbial mineral recovery. McGraw-Hill Book Co., Inc., New York.
12. **Rossi, G.** 1990. Biohydrometallurgy. McGraw-Hill Book Co. GmbH, Hamburg, Germany.
13. **Sohn, H. Y.** 1979. Fundamentals of the kinetics of heterogeneous reaction systems, p. 1–42. *In* H. Y. Sohn and M. E. Wadsworth (ed.), Rate processes of extractive metallurgy. Plenum Press, Inc., New York.
14. **Tuovinen, O. H., B. C. Kelley, and S. N. Groudev.** 1991. Mixed cultures in biological leaching processes and mineral biotechnology, p. 373–427. *In* J. G. Zeikus and E. A. Johnson (ed.), Mixed cultures in biotechnology. McGraw-Hill Book Co., Inc., New York.
15. **Wadsworth, M. E.** 1979. Hydrometallurgical processes, p. 133–241. *In* H. Y. Sohn and M. E. Wadsworth (ed.), Rate processes of extractive metallurgy. Plenum Press, Inc., New York.